

Enzymatic Transformation of Phosphate Decorated Magnetic Nanoparticles for Selectively Sorting and Inhibiting Cancer Cells

Xuwen Du,[†] Jie Zhou,[†] Liheng Wu,[‡] Shouheng Sun,[‡] and Bing Xu^{*,†}

[†]Department of Chemistry, Brandeis University, Waltham, Massachusetts 02454, United States

[‡]Department of Chemistry, Brown University, Providence, Rhode Island 02912, United States

S Supporting Information

ABSTRACT: As an important and necessary step of sampling biological specimens, the separation of malignant cells from a mixed population of cells usually requires sophisticated instruments and/or expensive reagents. For health care in the developing regions, there is a need for an inexpensive sampling method to capture tumor cells for rapid and accurate diagnosis. Here we show that an underexplored generic difference—overexpression of ectophosphatases—between cancer and normal cells triggers the D-tyrosine phosphate decorated magnetic nanoparticles ($\text{Fe}_3\text{O}_4\text{-p(D-Tyr)}$) to adhere selectively on cancer cells upon catalytic dephosphorylation, which enables magnetic separation of cancer cells from mixed population of cells (e.g., cocultured cancer cell (HeLa-GFP) and stromal cells (HS-S)). Moreover, the $\text{Fe}_3\text{O}_4\text{-p(D-Tyr)}$ nanoparticles also selectively inhibit cancer cells in the coculture. As a general method to broadly target cancer cells without highly specific ligand–receptor interactions (e.g., antibodies), the use of an enzymatic reaction to spatiotemporally modulate the state of various nanostructures in cellular environments will ultimately lead to the development of new theranostic applications of nanomaterials.



This communication reports the application of enzymatic transformation (ET) of a simple amino acid (*D*-tyrosine phosphate) decorated magnetic nanoparticles for selectively sorting and inhibiting cancer cells. Cell sorting, the isolation of certain types of cells from mixed cell population of organs or tissues, has become an increasingly important sampling method that has already contributed to many advances in biology and medicine.^{1,2} While the capture of bacteria is relatively easy by the magnetic nanoparticles decorated by a readily accessible ligand (e.g., vancomycin),³ the sorting of mammalian cells requires more complicated and expensive instruments and reagents. Fluorescent activated cell sorting (FACS),⁴ the most widely used cell sorting method, uses expensive hardware and requires labeling the cells of interest by fluorescent antibodies or cellular proteins.^{2,5} The current magnetic cell sorting still requires cell specific antibodies to be conjugated to the magnetic beads, which is a less well-defined process due to the nonspecific binding of proteins to the beads. Moreover, the development of inexpensive cell sorting method, without using expensive instrument (e.g., FACS) and/or reagents (e.g., antibodies), will contribute to low-cost diagnostics, which would be particularly attractive for developing regions that lack resources.⁶

Encouraged by the seminal work on the DNA linked gold nanoparticles to report DNA hybridization⁷ and the recent work on the dispersion of peptide coated gold nanoparticles to detect a specific enzyme,⁸ and based on our unexpected observation of selective formation of pericellular nanonets on cancer cells upon dephosphorylation of D-peptides catalyzed by ectophosphatases,⁹ we decide to use ET to trigger the adhesion of iron oxide nanoparticles on cells for sorting cancer cells. We

choose enzymatic reactions over antibodies to distinguish cancer and normal cells for three reasons: (i) the overexpression of ectophosphatases on the surface of cancer cells represents a generic difference between many cancer and normal cells;^{10,11} (ii) the omission of antibodies reduces the cost and increases the stability of agents; (iii) being highly efficient and specific, enzymatic reactions offer a simple, fast, yet fundamentally new way to modulate the surface chemistry of magnetic nanoparticles¹² for spatiotemporally defining the magnetic nanoparticles in cellular environment, which is less explored.

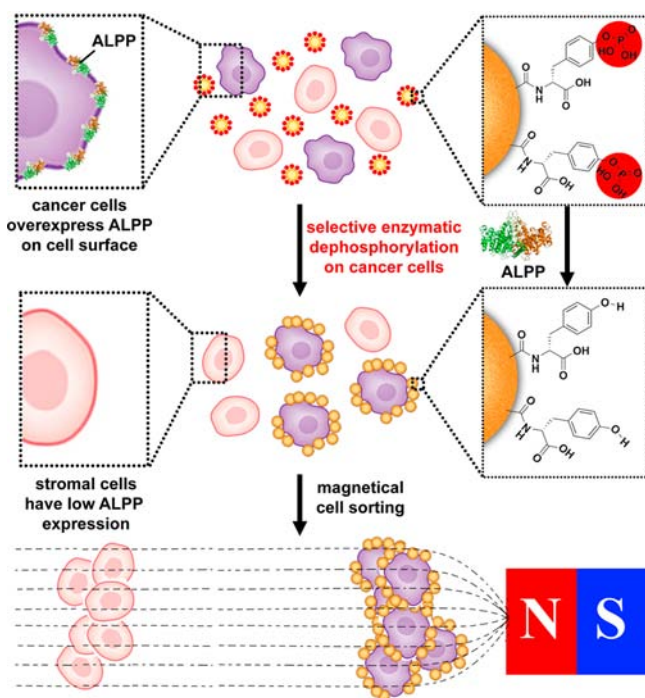
As illustrated in Scheme 1, we decorate iron oxide nanoparticles with a simple amino acid, *D*-tyrosine phosphate, to engineer the biofunctional magnetic nanoparticle ($\text{Fe}_3\text{O}_4\text{-p(D-Tyr)}$, MNP_pY). Ectophosphatases (e.g., placental alkaline phosphatase (ALPP) overexpressed on the surface of cancer cells¹¹) catalytically dephosphorylate the phosphate-bearing magnetic nanoparticles (MNP_pY) to form tyrosine coated magnetic nanoparticles ($\text{Fe}_3\text{O}_4\text{-(D-Tyr)}$, MNP_Y). Our microscopic studies confirm that, upon enzymatic transformation, MNP_Ys adhere selectively on the surface of cancer cells, which allows a small magnet to capture the cancer cells from a mixture of cancer and stromal cells (Scheme 2). Moreover, cell viability study indicates that MNP_pY selectively inhibits the growth of cancer cells (e.g., HeLa-GFP), with an IC_{50} of 12 $\mu\text{g/mL}$, in the coculture that mimics tumor microenvironment.¹³ As a new approach for selectively targeting and sorting cancer

Received: November 10, 2014

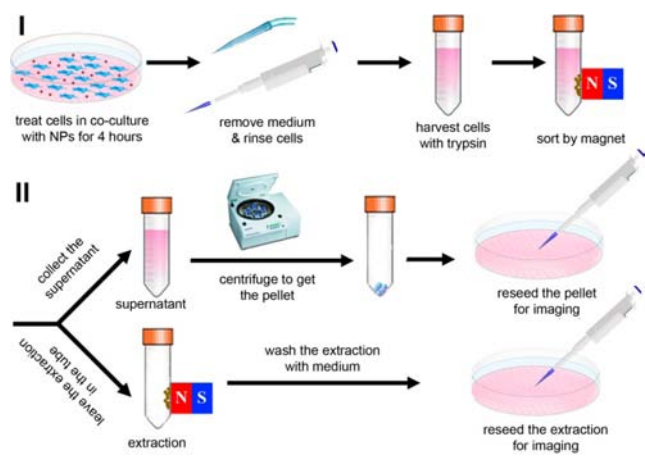
Revised: November 27, 2014

Published: November 28, 2014

Scheme 1. Enzymatic Transformation of Magnetic Nanoparticles for Selectively Sorting Cancer Cells



Scheme 2. Procedure for Separating the Cancer Cells from a Coculture of Cancer and Stromal Cells



cells, this exceptionally simple method not only illustrates a straightforward, selective, and inexpensive procedure for sorting cancer cells, but will also lead to the application of nanoparticles, based on the spatiotemporal distribution of a specific enzyme, for disease diagnosis and treatment.

The synthesis of MNP_pY is fast and straightforward: We directly modify the well-established iron oxide nanoparticles,¹⁴ which are surface-functionalized with oleic acid groups and commercially available,¹⁵ with D-tyrosine phosphate by using N-hydroxysuccinimide (NHS). After rinsing three times with methanol and water, respectively, we can collect the final MNP_pY with centrifugation and disperse them in water for use. Transmission electron microscopy confirms that there is little morphological change in the iron oxide nanoparticles before and after functionalization by D-tyrosine phosphates (Supporting Information Figure S1¹⁵). The quantification of phosphate on MNP_pY by using the phosphate assay indicates

that, on average, there are at least 124 D-tyrosine phosphate molecules on each MNP_pY nanoparticle (Supporting Information Figure S2¹⁵).

As shown in stage I in Scheme 2, the sorting of cancer cells from the cell mixture is exceptionally simple. After seeding about 1.0×10^6 HeLa-GFP¹⁶ and HS-5¹⁷ cells per culture dish (6 cm) overnight, we add MNP_pY (40 $\mu\text{g}/\text{mL}$) to incubate the coculture cells for 4 h. After removing the growth medium containing nanoparticles and rinsing the cells three times, we use trypsin solution (0.25% (w/v) in 0.53 mM EDTA) to detach the cells. Following aspiration of the cells to obtain the cell suspension by gently pipetting, we place a small magnet outside the Eppendorf tube for 1 min to divide the cell suspension into two portions: supernatant and extraction. After centrifugation and rinsing of the supernatant or extraction, the pellets of cells are reseeded onto confocal Petri dishes (stage II, Scheme 2) for imaging which acts as a way to verify the results of the sorting.

Figure 1 shows the results of the sorting of HeLa-GFP cells from the coculture of HeLa-GFP and HS-5 cells that mimics

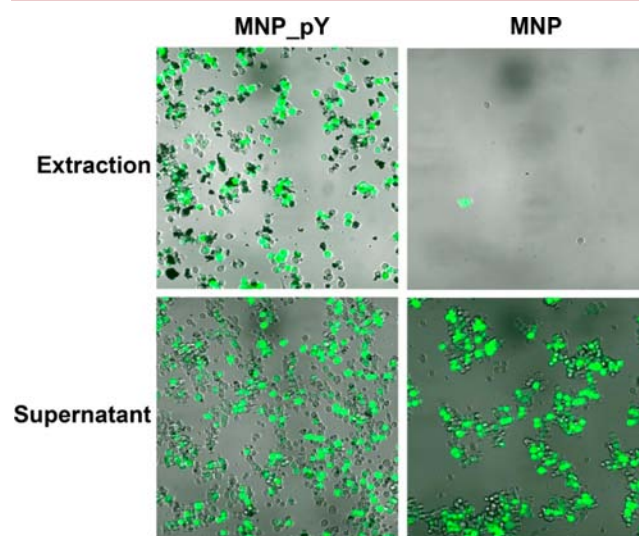


Figure 1. Overlaid bright field and fluorescent images (20 \times dry objective lens) of the extraction and supernatant portions of cells after adding MNP_pY (Left) and MNP (Right) to the coculture of HeLa-GFP and HS-5 cells for magnetic sorting. Cells were incubated with the growth medium, Dulbecco's Modified Eagle Medium (DMEM), containing 40 $\mu\text{g}/\text{mL}$ nanoparticles for 4 h (top: the cells extracted by magnet; bottom: the cells remaining in supernatant). The initial number of cells is 1.0×10^6 per 6 cm culture dish. The scale bar is 100 μm .

tumor microenvironment.¹⁷ After the treatment by MNP_pY and the magnetic capture, most of the cells from the extraction portion exhibit bright green fluorescence, indicating that they are cancer cells (i.e., HeLa-GFP). Only few HS-5 cells exist in the extraction, which may result from the intercellular interactions between cancer cells and stromal cells. On the contrary, the majority of the cells from the supernatant lack green fluorescence, indicating that they are HS-5 stromal cells. The bright field images (Supporting Information Figure S3¹⁵) show that many magnetic nanoparticles (MNP_Y) adhere on the surface of the cancer cells extracted by the magnet, which likely result from the dephosphorylation of D-tyrosine phosphate on the iron oxide nanoparticles by the overexpressed ectophosphatases on the surface of cancer cells. To confirm that

ET is responsible for the capture of the cancer cells, we use MNP as a control and repeat the procedure shown in Scheme 2. After treatment by MNP and magnetic sorting, almost no cells are observed from the extraction portion after reseeded, but the corresponding supernatant (i.e., from the sample treated by MNP) contains (almost) all the fluorescent (HeLa-GFP) and nonfluorescent (HS-5) cells. In agreement with this observation, after the incubation of the cells with the control iron oxide nanoparticles (MNP), the bright field images reveal that none of the MNP adheres on the surface of cancer or stromal cells (Supporting Information Figure S3¹⁵). These results, together, indicate that MNP_pYs, being catalytically dephosphorylated by the ectophosphatases overexpressed on the cancer cells, are suitable for magnetically and selectively sorting cancer cells from coculture of cancer and stromal cells.

To further confirm the selectivity of MNP_pY toward cancer cells, we use HeLa-GFP and HS-5 cells, separately, as the control cells and repeat the procedure shown in Scheme 2. The overlaid bright field and fluorescent images in Figure 2A

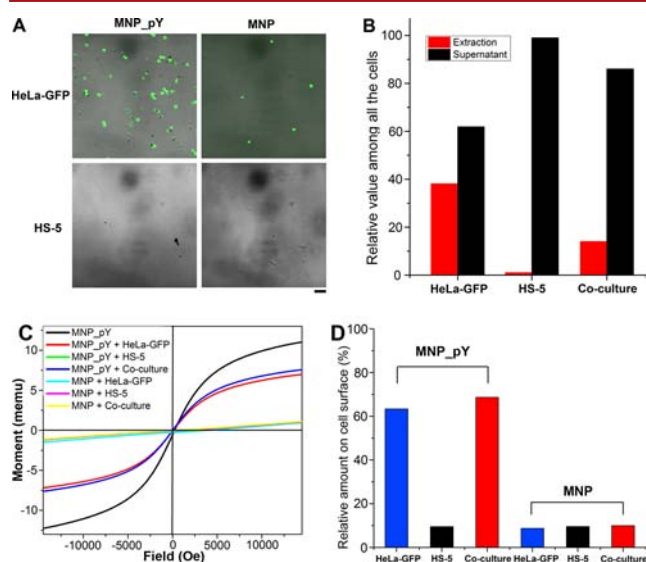


Figure 2. (A) Overlaid bright field and fluorescent microscopy images of the HeLa-GFP cells (top) and HS-5 cells (bottom) magnetically captured by incubating the cells with MNP_pY (left) and MNP (right). The scale bar is 100 μm . (B) The relative amount of cells (%) in the extraction or supernatant of all the cells collected after the treatment by 40 $\mu\text{g}/\text{mL}$ MNP_pY and the magnetic capture. (C) M–H curves of MNP_pY or MNP on the cells after incubation with HeLa-GFP, HS-5, or the coculture of HeLa-GFP and HS-5 cells. (D) Relative amounts of nanoparticles remaining on the cells.

indicate that, after the cells were incubated with MNP_pY and subjected to magnetic sorting, the extraction portion only contains HeLa-GFP cells (as proven by the bright green fluorescence from the cancer cells). The bright field images (Supporting Information Figure S4¹⁵) also confirm that MNP_pYs adhere on the surface of HeLa-GFP cells. The incubation of MNP_pY with HS-5 cells hardly results in HS-5 cells in the extraction portion, and there are no nanoparticles on the HS-5 cells in the supernatant (Supporting Information Figure S5¹⁵). Similar to the observation in the incubation of MNP with the coculture, the use of MNP on separately cultured HeLa-GFP or HS-5 captures neither GFP-HeLa nor HS-5 cells (Figure 2A) in the extractions.

To quantify the efficiency of cell capture of MNP_pY, we count the cell numbers in the extraction or the supernatant. As shown in Figure 2B, the addition of 100 μg of MNP_pY in the coculture of 6.6×10^5 total cells (with the initial ratio of HeLa-GFP and HS-5 cells in coculture to be 1:10), 14% of the cells are captured from the mixed cells, which indicates that this method separates over 90% of the cancer cells from the coculture. We reach this conclusion because (i) MNP_pY hardly leads to capture any HS-5 cells (i.e., less than 1%, Figure 2B); (ii) HeLa-GFP cells proliferate faster than HS-5 cells do; (iii) the addition of 100 μg of MNP_pY in the culture of initially 6.0×10^5 HeLa-GFP cells allows the capture of 3.0×10^5 cells (about 3000 cells/ μg MNP_pY, which is consistent with VSM measurement (*vide infra*)). In addition, to further demonstrate that ET of MNP_pY is the key factor for selective sorting of cancer cells, we utilize MNP_Y, which results from the treatment of MNP_pY with ALP, to incubate with cells and repeat the procedure shown in Scheme 2. According to cell viability test, MNP_Y itself shows little cytotoxicity to cells (Supporting Information Figure S6A¹⁵). As shown in Supporting Information Figure S6B,¹⁵ almost no cells are observed from the extraction portion while all cells remain in the corresponding supernatant (Supporting Information Figure S6C). These results confirm that, although the treatment of MNP_pY with phosphatases will generate MNP_Y, it is ET of MNP_pY by overexpressed ectophosphatases at the surface of cancer cells, not MNP_Y itself, that triggers the magnetic separation and selective inhibition of cancer cells from coculture circumstance.

We study magnetic properties of the iron oxide nanoparticles by using a vibrating sample magnetometer (VSM) for quantifying the amount of MNP_Y remaining on the cells. As shown in Figure 2C, 200 μg of MNP_pY has the magnetic moment of 11.0 memu, which can serve as a reference for estimating the magnetic nanoparticles on the cells. After incubation with coculture of HeLa-GFP and HS-5 cells with same amount of MNP_pY for 4 h, the magnetic moment of nanoparticles remaining on all of the cells is decreased to 7.6 memu, which is around 69% of all the MNP_pY before the treatment (Figure 2D). Moreover, when the MNP_pYs are incubated with only the HeLa-GFP cells, the moment of MNP_Y on the cell surface is 7.0 memu, suggesting that 63% of nanoparticles adhere to the HeLa-GFP cells. This quantity is comparable to the amount of MNP_Y on the HeLa-GFP in the coculture. On the other hand, the incubation of MNP_pY with HS-5 cells only results in the residue of the magnetic moment of 1.0 memu, which is 9% of all the MNP_pY before the treatment, thus confirming that HS-5 cells hardly absorb MNP_pY. These results are compatible with the optical images of the pellets collected with the treatment of nanoparticles (Supporting Information Figure S7¹⁵). According to cell numbers and the magnetic moments, we estimate the capture efficiency to be about 7000 cells/ μg MNP_pY, which is comparable to the efficiency obtained by counting numbers of captured cells. The measurement of the cells treated only by MNPs (Figure 2C and D) confirms that there are few control iron oxide nanoparticles (MNP) remaining on the surface of any cells. While nonselective internalization of MNPs by cells could lead to the reduction of selectivity, the use of D-tyrosine and relatively short incubation (4 h), in fact, minimizes the internalization of MNPs.

Besides selectively capturing cancer cells in coculture, MNP_pY selectively inhibits the proliferation of cancer cells.

As shown in Figure 3, being incubated with different concentrations of MNP_pY, the viability of coculture of

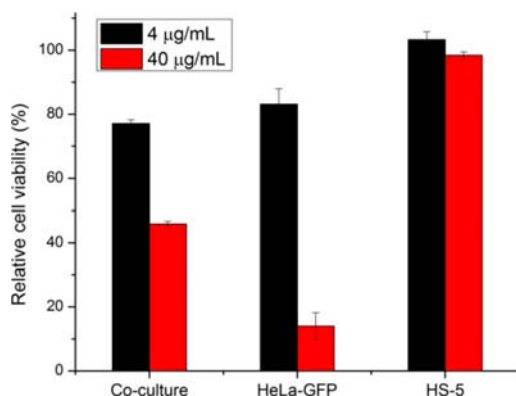


Figure 3. Relative cell viability (determined by counting the cell numbers; 100% represents the control, i.e., 0 µg/mL of the compound) of coculture of HeLa-GFP and HS-5 cells; HeLa-GFP cells; and HS-5 cells incubated with MNP_pY at the concentrations of 4 and 40 µg/mL. The initial number of cells is 1.0×10^4 /well.

HeLa-GFP and HS-5 cells (measured by counting the cell number) is much lower than that of the control. When the concentration is larger than 20 µg/mL, the cell viability remains almost the same, which indicates that the stromal cells are still alive while most of the cancer cells are killed by MNP_pY (Supporting Information Figure S8¹⁵). This result agrees with the viability of the homogeneous cells treated by MNP_pY. After being treated by different concentrations of MNP_pY, the proliferation of HeLa-GFP cells shows significant inhibition, especially when the concentration of MNP_pY is larger than 10 µg/mL. Cell viability study indicates that MNP_pY inhibits the growth of HeLa-GFP cells with the IC_{50} value of 12 µg/mL (10.2 µM tyrosine phosphate) at 48 h, which is comparable to that of cisplatin-loaded gold nanoparticles (6 µM).¹⁸ On the contrary, after being treated by the same concentrations of MNP_pY, HS-5 cells maintain almost the same level of proliferation with the control, which indicates that MNP_pY has little cytotoxicity to the stromal cells (e.g., HS-5). When HeLa-GFP cells are treated with 40 µg/mL of MNP_pY and different concentrations of L-phenylalanine (e.g., 1, 5, 10 mM), a known inhibitor of ALPP,¹⁹ more than 60% of cells are alive (Supporting Information Figure S9¹⁵). In addition, the incubation of MNP with HeLa-GFP or HS-5 cells hardly inhibits the cell proliferation (Supporting Information Figure S10¹⁵). These results indicate that ALPP is largely responsible for converting MNP_pY to MNP_Y on cancer cell surface for selectively sorting and inhibiting cancer cells.

In conclusion, this work, for the first time, demonstrates the use of enzymatic transformation (ET) of magnetic nanoparticles for selectively sorting and inhibiting cancer cells without involving specific ligand–receptor interactions or the use of antibodies. The high capture efficiency of cancer cells from the coculture demonstrates the expression level of enzymes as a new paradigm for exploring strategies that target cancer cells. While the overexpression of ectophosphatases (e.g., ALPP) represents a generic difference between cancer and normal cells, there are certain cancer cells expressing normal levels of ALPP to render MNP_pY ineffective. This apparent limitation should be solvable by identifying other genuine enzymatic differences between cancer and normal cells. This

strategy relies on a specific enzymatic reaction (e.g., catalytic dephosphorylation), but not specific enzyme inhibition, to target cancer cells selectively. The same principle should be useful for developing a relatively inexpensive, simple, and selective method for sampling other biological specimens. One of most intriguing aspect of this work is that MNP_Y only binds to cancer cells after enzymatic dephosphorylation by the ectophosphatases. We speculate that this enzyme activated binding (EAB) is either entropy favorable or associates with the conformation dynamics of the unknown protein complexes interacting with the MNP_Y, or possibly both. This previously unexplored mechanism undoubtedly warrants further investigation, which may lead to a new paradigm in multivalent binding. By mimicking the essence of biological signaling processes (e.g., kinase/phosphatase enzymatic switch²⁰), the use of enzymatic transformation to control the formation or state of nanostructures²¹ ultimately may lead to new approaches for detecting and treating other diseases.

■ ASSOCIATED CONTENT

● Supporting Information

Details of the phosphate assay, magnetic characterization, TEM images, confocal images, and cytotoxicity data. This material is available free of charge via the Internet at <http://pubs.acs.org>.

■ AUTHOR INFORMATION

Corresponding Author

*E-mail: bxu@brandeis.edu.

Notes

The authors declare no competing financial interest.

■ ACKNOWLEDGMENTS

This work was partially supported by the NIH (R01A142746) and an NSF MRSEC grant (DMR-0820492).

■ REFERENCES

- (1) Claros, M. G., and Vincens, P. (1996) *Eur. J. Biochem.* 241, 779.
- (2) Panyam, J., and Labhasetwar, V. (2003) *Adv. Drug Delivery Rev.* 55, 329.
- (3) Cormack, B. P., Valdivia, R. H., and Falkow, S. (1996) *Gene* 173, 33.
- (4) Xing, B. G., Yu, C. W., Chow, K. H., Ho, P. L., Fu, D. G., and Xu, B. (2002) *J. Am. Chem. Soc.* 124, 14846. Xing, B. G., Ho, P. L., Yu, C. W., Chow, K. H., Gu, H. W., and Xu, B. (2003) *Chem. Commun.*, 2224.
- (5) Liu, T.-Y.; Tsai, K.-T.; Wang, H.-H.; Chen, Y.; Chen, Y.-H.; Chao, Y.-C.; Chang, H.-H.; Lin, C.-H.; Wang, J.-K.; Wang, Y.-L. *Nat. Commun.* 2011, 2. Xing, B. G., Yu, C. W., Chow, K. H., Ho, P. L., Fu, D. G., and Xu, B. (2002) *J. Am. Chem. Soc.* 124, 14846.
- (6) Julius, M. H., Masuda, T., and Herzenbe, La (1972) *Proc. Natl. Acad. Sci. U.S.A.* 69, 1934. Kreth, H. W., and Herzenbe, La (1974) *Cellular Immunol.* 12, 396.
- (7) Orlic, D., Kajstura, J., Chimenti, S., Jakoniuk, I., Anderson, S. M., Li, B. S., Pickel, J., McKay, R., Nadal-Ginard, B., Bodine, D. M., Leri, A., and Anversa, P. (2001) *Nature* 410, 701.
- (8) Martinez, A. W., Phillips, S. T., Whitesides, G. M., and Carrilho, E. (2010) *Anal. Chem.* 82, 3. Martinez, A. W., Phillips, S. T., Wiley, B. J., Gupta, M., and Whitesides, G. M. (2008) *Lab Chip* 8, 2146.
- (9) Sia, S. K., Linder, V., Parviz, B. A., Siegel, A., and Whitesides, G. M. (2004) *Angew. Chem., Int. Ed.* 43, 498.
- (10) Kuo, J. S., Kuyper, C. L., Allen, P. B., Fiorini, G. S., and Chiu, D. T. (2004) *Electrophoresis* 25, 3796.
- (11) Mirkin, C. A., Letsinger, R. L., Mucic, R. C., and Storhoff, J. J. (1996) *Nature* 382, 607. Rosi, N. L., and Mirkin, C. A. (2005) *Chem. Rev.* 105, 1547.

- (8) Jia, J. B., Wang, B. Q., Wu, A. G., Cheng, G. J., Li, Z., and Dong, S. J. (2002) *Anal. Chem.* 74, 2217. Liu, J. W., and Lu, Y. (2003) *J. Am. Chem. Soc.* 125, 6642. Laromaine, A., Koh, L. L., Murugesan, M., Ulijn, R. V., and Stevens, M. M. (2007) *J. Am. Chem. Soc.* 129, 4156.
- (9) Kuang, Y., Shi, J., Li, J., Yuan, D., Alberti, K. A., Xu, Q., and Xu, B. (2014) *Angew. Chem., Int. Ed.* 53, 8104.
- (10) Fishman, W. H., Inglis, N. R., Green, S., Anstiss, C. L., Gosh, N. K., Reif, A. E., Rustigia, R., Krant, M. J., and Stolbach, L. L. (1968) *Nature* 219, 697.
- (11) Pospisil, P., Iyer, L. K., Adelstein, S. J., and Kassis, A. I. (2006) *BMC Bioinformatics* 7, 11.
- (12) Xu, C. J., Xu, K. M., Gu, H. W., Zheng, R. K., Liu, H., Zhang, X. X., Guo, Z. H., and Xu, B. (2004) *J. Am. Chem. Soc.* 126, 9938.
- (13) Hanahan, D., and Weinberg, R. A. (2011) *Cell* 144, 646.
- (14) Sun, S. H., Zeng, H., Robinson, D. B., Raoux, S., Rice, P. M., Wang, S. X., and Li, G. X. (2004) *J. Am. Chem. Soc.* 126, 273. Hyeon, T., Lee, S. S., Park, J., Chung, Y., and Bin Na, H. (2001) *J. Am. Chem. Soc.* 123, 12798.
- (15) Xu, B. Supporting Information.
- (16) Platani, M., Goldberg, I., Swedlow, J. R., and Lamond, A. I. (2000) *J. Cell Biol.* 151, 1561.
- (17) McMillin, D. W., Delmore, J., Weisberg, E., Negri, J. M., Geer, D. C., Klippel, S., Mitsiades, N., Schlossman, R. L., Munshi, N. C., Kung, A. L., Griffin, J. D., Richardson, P. G., Anderson, K. C., and Mitsiades, C. S. (2010) *Nat. Med.* 16, 483.
- (18) Wang, X., Cai, X., Hu, J., Shao, N., Wang, F., Zhang, Q., Xiao, J., and Cheng, Y. (2013) *J. Am. Chem. Soc.* 135, 9805.
- (19) Fernley, H. N., and Walker, P. G. (1970) *Biochem. J.* 116, 543.
- (20) Lodish, H., Berk, A., Kaiser, C. A., Krieger, M., Scott, M. P., Bretscher, A., Ploegh, H., and Matsudaira, P. (2012) *Molecular Cell Biology*, 7th ed., W. H. Freeman.
- (21) Zhou, J., Du, X., Gao, Y., Shi, J., and Xu, B. (2014) *J. Am. Chem. Soc.* 136, 2970. Yang, Z., Ho, P.-L., Liang, G., Chow, K. H., Wang, Q., Cao, Y., Guo, Z., and Xu, B. (2007) *J. Am. Chem. Soc.* 129, 266. Yang, Z. M., and Xu, B. (2004) *Chem. Commun.*, 2424. Lovell, J. F., Jin, C. S., Huynh, E., MacDonald, T. D., Cao, W., and Zheng, G. (2012) *Angew. Chem., Int. Ed.* 51, 2429. Kim, J., Lee, J. E., Lee, J., Yu, J. H., Kim, B. C., An, K., Hwang, Y., Shin, C. H., Park, J. G., Kim, J., and Hyeon, T. (2006) *J. Am. Chem. Soc.* 128, 688. Lee, J.-H., Huh, Y.-M., Jun, Y.-w., Seo, J.-w., Jang, J.-t., Song, H.-T., Kim, S., Cho, E.-J., Yoon, H.-G., Suh, J.-S., and Cheon, J. (2007) *Nat. Med.* 13, 95. Zhao, Y., Chen, Z., Chen, Y., Xu, J., Li, J., and Jiang, X. (2013) *J. Am. Chem. Soc.* 135, 12940. Xia, Y. N., Yang, P. D., Sun, Y. G., Wu, Y. Y., Mayers, B., Gates, B., Yin, Y. D., Kim, F., and Yan, Y. Q. (2003) *Adv. Mater.* 15, 353. Jin, Y., and Gao, X. (2009) *Nat. Nanotechnol.* 4, 571. Yang, J., Dave, S. R., and Gao, X. (2008) *J. Am. Chem. Soc.* 130, 5286. Ku, T.-H., Chien, M.-P., Thompson, M. P., Sinkovits, R. S., Olson, N. H., Baker, T. S., and Gianneschi, N. C. (2011) *J. Am. Chem. Soc.* 133, 8392.